

# Operational Runtime Behavior Mining for Open-Source Supply Chain Security

Zhuoran Tan, Ke Xiao, Jeremy Singer, Christos Anagnostopoulos\*

University of Glasgow

Glasgow, UK

[z.tan.1,k.xiao.1,jeremy.singer,Christos.Anagnostopoulos}@glasgow.ac.uk](mailto:z.tan.1,k.xiao.1,jeremy.singer,Christos.Anagnostopoulos}@glasgow.ac.uk)

## Abstract

Open-source software (OSS) is a critical component of modern software systems, yet supply chain security remains challenging in practice due to unavailable or obfuscated source code. Consequently, security teams often rely on runtime observations collected from sandboxed executions to investigate suspicious third-party components. We present HeteroGAT-Rank, an industry-oriented runtime behavior mining system that supports analyst-in-the-loop supply chain threat investigation. The system models execution-time behaviors of OSS packages as lightweight heterogeneous graphs and applies attention-based graph learning to rank behavioral patterns that are most relevant for security analysis. Rather than aiming for fully automated detection, HeteroGAT-Rank surfaces actionable runtime signals—such as file, network, and command activities—to guide manual investigation and threat hunting.

To operate at ecosystem scale, the system decouples offline behavior mining from online analysis and integrates parallel graph construction for efficient processing across multiple ecosystems. An evaluation on a large-scale OSS execution dataset shows that HeteroGAT-Rank effectively highlights meaningful and interpretable behavioral indicators aligned with real-world vulnerability and attack trends, supporting practical security workflows under realistic operational constraints.

## CCS Concepts

- Computing methodologies → **Graph learning**; Heterogeneous learning;
- Information systems → **Knowledge graphs**;
- Security and privacy → Supply chain threats.

## Keywords

Open-Source Software Security, Software Supply Chain, Runtime Behavior Analysis, Sandbox-based Analysis, Threat Hunting

## ACM Reference Format:

Zhuoran Tan, Ke Xiao, Jeremy Singer, Christos Anagnostopoulos. 2026. Operational Runtime Behavior Mining for Open-Source Supply Chain Security. In *Companion Proceedings of the 34th ACM Symposium on the Foundations*

\*Zhuoran Tan is the corresponding author.

Permission to make digital or hard copies of all or part of this work for personal or classroom use is granted without fee provided that copies are not made or distributed for profit or commercial advantage and that copies bear this notice and the full citation on the first page. Copyrights for components of this work owned by others than the author(s) must be honored. Abstracting with credit is permitted. To copy otherwise, or republish, to post on servers or to redistribute to lists, requires prior specific permission and/or a fee. Request permissions from [permissions@acm.org](mailto:permissions@acm.org).

FSE '26, Montréal, QC, Canada

© 2026 Copyright held by the owner/author(s). Publication rights licensed to ACM.

ACM ISBN 978-x-xxxx-xxxx-x/YY/MM

<https://doi.org/10.1145/nnnnnnn.nnnnnnn>

of Software Engineering (FSE '26), July 5–9, 2026, Montreal, Canada. ACM, New York, NY, USA, 12 pages. <https://doi.org/10.1145/nnnnnnn.nnnnnnn>

## 1 Introduction

Open-source software (OSS) underpins modern systems, making software supply chain security a growing operational concern. Graph-based representations such as ASTs, CFGs, and dependence graphs are effective for vulnerability analysis when source code is available [17, 21, 36, 49]. In practice, however, code is often unavailable, incomplete, or obfuscated, limiting the applicability of static analysis [20]. Moreover, many supply chain attacks only manifest through runtime behaviors (e.g., multi-stage execution and environment-dependent logic) that are difficult to infer from code alone [42]. As a result, security teams increasingly rely on dynamic evidence from execution monitoring, especially in closed-source and confidential environments where runtime traces may be the only viable signal [3].

A key operational challenge is scale: execution tracing produces large volumes of noisy events, and analysts must quickly identify which runtime activities are most relevant for threat hunting. We therefore focus on enabling an *operational understanding of runtime behavior* from traces alone: rather than reconstructing program logic, we aim to prioritize suspicious behaviors such as unexpected file access, network communication, and command execution in a form that supports analyst-in-the-loop triage.

We study this setting using the OSPTrack dataset [41], which contains labeled runtime execution features collected from sandboxed runs of open-source packages across five ecosystems. We represent execution traces as lightweight heterogeneous graphs, where each software instance is modeled as a star-shaped subgraph rooted at a package node and connected to runtime entities such as file paths, sockets, DNS hosts, and executed commands. This one-hop design captures direct interactions between a package and its environment while balancing expressiveness, scalability, and interpretability under industrial constraints.

To analyze these graphs, we propose **HeteroGAT-Rank**, an attention-based heterogeneous graph learning framework built on type-aware GATv2 attention [5]. HeteroGAT-Rank learns to rank runtime entities and edges by relevance to supply chain threat analysis, producing instance-specific pivots that analysts can validate in sandbox logs and translate into hunting queries.

In summary, this paper makes the following contributions<sup>1</sup>:

<sup>1</sup>The HeteroGAT-Rank code is available at [1] to facilitate reproducibility and further research.

- We present an industry-oriented framework for mining actionable runtime behavioral indicators from sandboxed executions of open-source software to support supply chain security analysis.
- We propose a scalable pipeline that transforms dynamic execution data into heterogeneous graph representations across multiple ecosystems, enabling cross-ecosystem behavioral analysis.
- We develop **HeteroGAT-Rank**, an attention-based graph learning system that prioritizes runtime behaviors for analyst-in-the-loop investigation under realistic operational constraints.
- We provide an empirical evaluation and case studies demonstrating how ranked behavioral indicators can support practical threat hunting and security workflows.

## 2 Literature Review

This work builds on prior research in software security and supply chain analysis that leverages structured representations and learning-based techniques to extract security-relevant signals. Under realistic operational constraints, related efforts broadly fall into (i) feature representation and prioritization, and (ii) supply chain security techniques based on static or dynamic analysis.

### 2.1 Feature Representation and Prioritization

Learning-based representation has been explored to support security analysis. Yin et al. [47] proposed a modality-aware graph convolutional framework to embed heterogeneous vulnerability attributes and mitigate sparsity via transfer learning, demonstrating the value of structured representations but primarily targeting offline vulnerability analysis. Luo et al. [23] studied online feature selection in high-velocity streams to improve efficiency; however, such methods typically operate on flat feature spaces and offer limited support for reasoning over structured runtime behaviors. Differential analysis has also been used to reveal localized malicious modifications: Froh et al. [8] and Barr et al. [3] show that fine-grained differences in package updates or binaries can expose malicious changes, yet these approaches rely on paired versions/baselines and do not directly address ecosystem-scale aggregation of runtime behaviors. In contrast, our work treats learning-based ranking as an operational aid: we surface instance-specific runtime pivots for investigation, rather than optimizing predictive performance in isolation.

### 2.2 Software Supply Chain Security

Many supply chain defenses rely on static code analysis or controlled dynamic testing. Zheng et al. [52] proposed OSCAR, a dynamic code-poisoning detection pipeline for NPM and PyPI; while effective, its per-sample simulation and fuzzing can limit scalability in large ecosystems. Other approaches are source-code-centric: Zhang et al. [49] use property graphs with BERT-based embeddings for function-level vulnerability detection, and Zhang et al. [51] combine program slicing with GRU-based models and vulnerability dictionaries to capture recurring patterns. These techniques perform well when source code is available but are less suitable for obfuscated or closed-source components and cannot capture behaviors

that only manifest during execution. In contrast, we focus on sandboxed runtime behavior as an operational data source and adopt lightweight heterogeneous graphs to support analyst-in-the-loop investigation across ecosystems; HeteroGAT-Rank complements existing detection tools by prioritizing actionable runtime signals for threat hunting and manual analysis.

## 3 Methodology

Our framework has two components (Figures 1 and 3): (1) we construct a per-package heterogeneous behavior graph from sandbox runtime traces; and (2) we train an attention-based GNN on a supervised subgraph classification task and reuse node/edge attentions for differential feature ranking.

**Per-package heterogeneous subgraph.** For each package, we build a directed heterogeneous subgraph  $G_r = (V_r, E_r)$  rooted at the package node  $v_{\text{pkg}}$ . Nodes and edges are typed (e.g., Path, DNS, CMD, Socket and their relations), capturing the package's runtime footprint within one hop from  $v_{\text{pkg}}$ . Each node  $i \in V_r$  has an initial feature vector  $h_i \in \mathbb{R}^d$  (e.g., embedded token/value features).

**Learning and interpretability signals.** Each subgraph  $G_r$  is paired with a binary label  $y_r \in \{0, 1\}$  (e.g., malicious vs. benign). We learn a predictor  $f(G_r) \rightarrow \hat{y}_r$  using type-aware attention message passing and pooling to obtain a subgraph embedding  $Z_r$ . During training/inference, we record node/edge attention scores (e.g.,  $\alpha_{ij}^\phi$ ) as lightweight interpretability signals, which are then used by our differential analysis module to surface high-impact indicators.

### 3.1 Dataset Description

**Base dataset** For the dataset we use in this project, we build on the published cross-ecosystem runtime-trace dataset [41], collected using the OpenSSF Package Analysis framework [13] as shown in top part of Figure 1. The framework executes open-source packages inside isolated sandboxes to simulate both the installation and runtime (import) phases, while monitoring dynamic behaviors including file I/O events, network socket activities, executed commands, and DNS requests. The released dataset spans five ecosystems—Rust (crates.io), JavaScript (NPM), PHP (packagist), Python (PyPI), and Ruby (rubygems). Sandbox execution, trace logging, and the labeling protocol for the base portion are provided by the original dataset authors and are not contributions of this paper.

**Our extension (additional malicious instances).** To improve coverage of malicious behaviors for downstream modeling, we extend the dataset by replaying the same OpenSSF collection pipeline and applying the same labeling criteria as the base dataset, producing additional malicious instances under a consistent schema. The resulting final dataset contains 9,758 instances. Table 1 summarizes the ecosystem-level statistics.

**What we treat as “source data” in this paper.** Each instance provides structured, phase-specific runtime observations (e.g., file paths with access actions, DNS hosts with query types, socket-related endpoints/hosts/ports, and executed command strings). Our contribution starts from these published and extended structured logs: we deterministically map them into a unified heterogeneous knowledge graph schema for cross-ecosystem behavior modeling.

**Cross-ecosystem learning and imbalance.** The dataset exhibits notable label imbalance across ecosystems (Table 1), reflecting

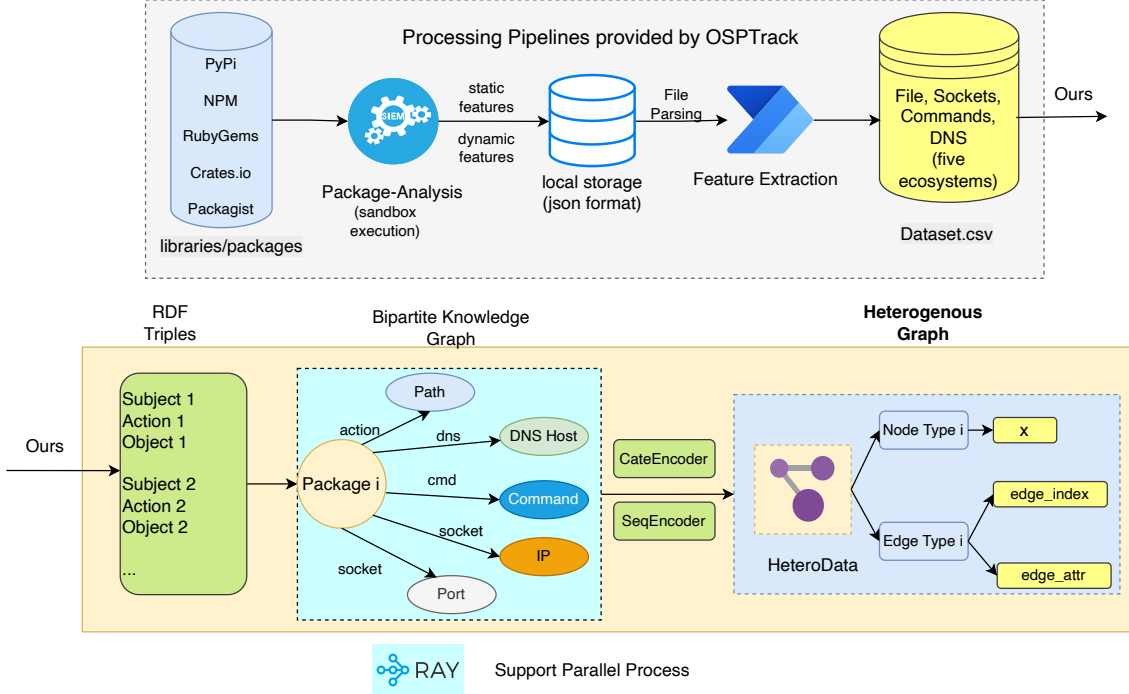


Figure 1: Knowledge Graph Construction Pipeline

Table 1: Ecosystem Package Count by Label

Ecosystem	Package Count	Malicious
crates.io	1206	1 (0.1%)
npm	5773	1128 (19.5%)
packagist	265	0 (0.0%)
pypi	2176	853 (39.2%)
rubygems	338	277 (81.9%)
<b>Total</b>	<b>9758</b>	<b>2259 (23.1%)</b>

real-world differences in attack prevalence and reporting practices. Rather than balancing labels within each ecosystem, we adopt a cross-ecosystem learning setup in which all ecosystems are jointly modeled. This reduces ecosystem-specific shortcuts by encouraging the model to focus on behavior patterns that generalize across ecosystems. To further mitigate bias, ecosystem identifiers are not used as predictive features, and evaluation emphasizes feature-level behavior analysis rather than per-ecosystem accuracy.

**Compute environment.** Graph construction is CPU/RAM intensive, whereas representation learning and downstream training are GPU intensive. To optimize resource usage and improve pipeline efficiency, we decouple graph construction from training and stream serialized subgraphs during training. Hardware and container details are provided in the artifact repository for reproducibility.

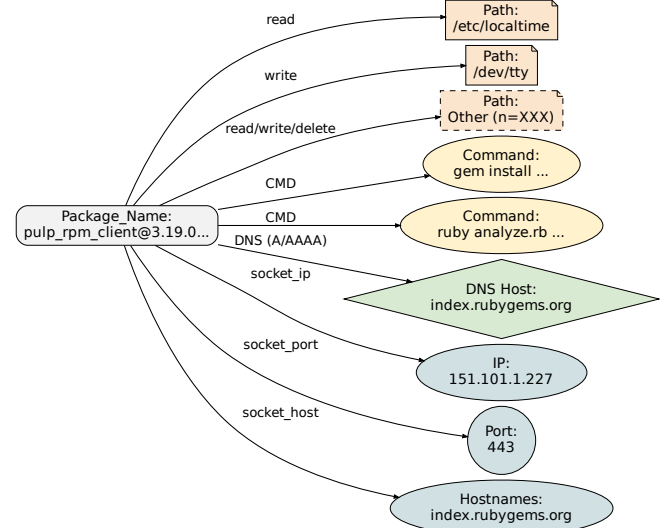


Figure 2: Record-to-Graph Example

### 3.2 Knowledge Graph Creation

To analyze runtime behaviors across ecosystems, we transform raw sandbox execution traces into heterogeneous subgraphs that represent each package's behavioral footprint. The pipeline, summarized in bottom part of Figure 1, converts feature logs (file I/O,

network, command execution, DNS requests, etc.) into a consistent graph structure suitable for heterogeneous GNN analysis. Figure 2 provides a worked example from the published trace dataset (and our extension follows the same protocol), illustrating how a single instance record is mapped into our one-hop star-shaped subgraph with typed edges.

**3.2.1 Behavior-to-Graph Transformation.** Each software instance is represented as a one-hop star-shaped subgraph  $G = (V, E)$ , rooted at a `Package_Name` node (Figure 2). The leaves correspond to observed runtime entities such as file paths, commands, or network hosts. In the worked example, the package node connects to representative path, DNS, command, and socket entities; long-tail objects are collapsed for readability. Edges denote typed interactions between the package and its environment, including:

- `Package_Name`  $\xrightarrow{\text{Action}}$  `Path`
- `Package_Name`  $\xrightarrow{\text{DNS}}$  `DNS Host`
- `Package_Name`  $\xrightarrow{\text{CMD}}$  `Command`
- `Package_Name`  $\xrightarrow{\text{Socket}}$  `Endpoint (IP/Port/Hostname)`

where the `Action` represents ‘write’, ‘delete’, or ‘read’. The `DNS` indicates the DNS types: ‘AAAA’, ‘A’, or ‘CNAME’.

This design captures direct environmental interactions rather than multi-hop control flows, providing a concise but expressive view of how a package behaves at runtime.

Raw string values (e.g., paths or domain names) are normalized and encoded into semantic embeddings using lightweight categorical and transformer-based encoders [45]. This preserves meaning similarity between behavior tokens (e.g., `/tmp/install.sh`  $\approx$  `/var/install.sh`) while reducing sparsity across ecosystems.

**3.2.2 Parallel Construction and Alignment.** The dataset comprises 9,758 instances spanning five ecosystems (Python, JavaScript, Ruby, PHP, Rust). To process these at scale, we parallelize graph generation and feature encoding across CPUs, producing over 10 million nodes and 54 million edges. Graphs are stored in PyG HeteroData [7] format for efficient training.

To enable mini-batch learning, we align subgraphs by type and dimension, ensuring each batch maintains consistent node and edge representations. Instead of describing low-level padding or indexing, we emphasize semantic consistency—every node and relation keeps its behavioral type so that learned attention weights remain interpretable across ecosystems.

**3.2.3 Operationally Interpretable Runtime Graphs.** Unlike traditional source-code graphs [4, 28], these runtime knowledge graphs explicitly encode observable actions that analysts can interpret. The one-hop structure highlights *what the package did* rather than *how it was implemented*, aligning model outputs with behavioral comprehension. When attention scores are later extracted, the same schema supports practical investigation by surfacing dominant runtime patterns—for example, unexpected network communication or file modifications. Overall, this stage converts heterogeneous runtime traces into interpretable graph representations, preserving semantic fidelity for learning while remaining actionable for downstream security analysis.

### 3.3 HeteroGAT-Rank Framework

The HeteroGAT-Rank framework, as shown in Figure 3, builds upon GATv2Conv and extends it to heterogeneous graph settings by stacking multiple layers of type-aware attention-based convolution, followed by a normalization layer (LayerNorm) and an attention-guided pooling mechanism. Due to small batch size setting up, LayerNorm is implemented to stabilize the training process. The model integrates both node-level and edge-level attention scores, which are extracted and ranked to reflect their relative importance in the prediction process. Those extracted features can be supplied for further threat hunting process. The detailed information is provided in following subsections.

**3.3.1 Model Architecture.** We design a heterogeneous graph attention network for subgraph-level classification, explicitly modeling semantic diversity across node and edge types. The backbone stacks type-aware HeteroConv layers with GATv2Conv over a fixed set of typed, directed relations. Unlike homogeneous GNNs, each relation is parameterized separately to preserve directionality and inter-type dependencies. We adopt multi-head attention per relation to capture diverse semantic interactions; attention heads are then concatenated and passed to the next layer.

To mitigate unnecessary computation and index mapping overheads, we ignore aggregation *into* `Package_Name` nodes, which function purely as sources. This structural simplification maintains semantic integrity without introducing noise from trivial root nodes. To improve convergence and optimization stability, each GATv2 layer is followed by LayerNorm, preparing features for subsequent attention-based pooling.

**3.3.2 Attention Pooling.** We use a two-stage attention-based pooling mechanism to construct compact subgraph representations tailored to heterogeneous inputs. Unlike Global Mean or Max Pooling [12, 19], attention pooling emphasizes salient substructures using learned importance scores. Inspired by masked representation learning [18, 33] and attentive pooling [50], we extract top- $k$  nodes (and their incident edges) according to attention-derived scores, yielding a compact behavioral fingerprint that remains interpretable for analyst-in-the-loop triage.

Unlike DiffPool [48], whose hierarchical clustering is unnecessary and ill-suited for our 1-hop subgraph structure, we adopt a flat pooling design. We then aggregate pooled node and edge representations (e.g., by attention-weighted sum) and concatenate them to form the final subgraph embedding used for classification.

**3.3.3 Ensemble Loss.** The goal of training is not only detection accuracy but also *actionable* evidence that is stable and compact across ecosystems. Optimizing classification alone can yield diffuse attention patterns that are harder to operationalize. We therefore introduce a CompositeLoss that balances correctness, representation separability, decisiveness of attributions, and compactness of selected evidence:  $\mathcal{L}_{\text{total}} = \lambda_{\text{cls}} \cdot \mathcal{L}_{\text{cls}} + \lambda_{\text{ctr}} \cdot \mathcal{L}_{\text{contras}} + \lambda_{\text{ent}} \cdot \mathcal{L}_{\text{entropy}} + \lambda_{\text{sp}} \cdot \mathcal{L}_{\text{sparsity}}$ , where  $\mathcal{L}_{\text{cls}}$  is cross-entropy for subgraph labels;  $\mathcal{L}_{\text{contras}}$  improves cross-ecosystem robustness by separating embeddings with standard negative sampling practices [31];  $\mathcal{L}_{\text{entropy}}$  discourages overly uniform attention to make evidence selection more decisive; and  $\mathcal{L}_{\text{sparsity}}$  promotes compact top- $k$  evidence that is easier to inspect.

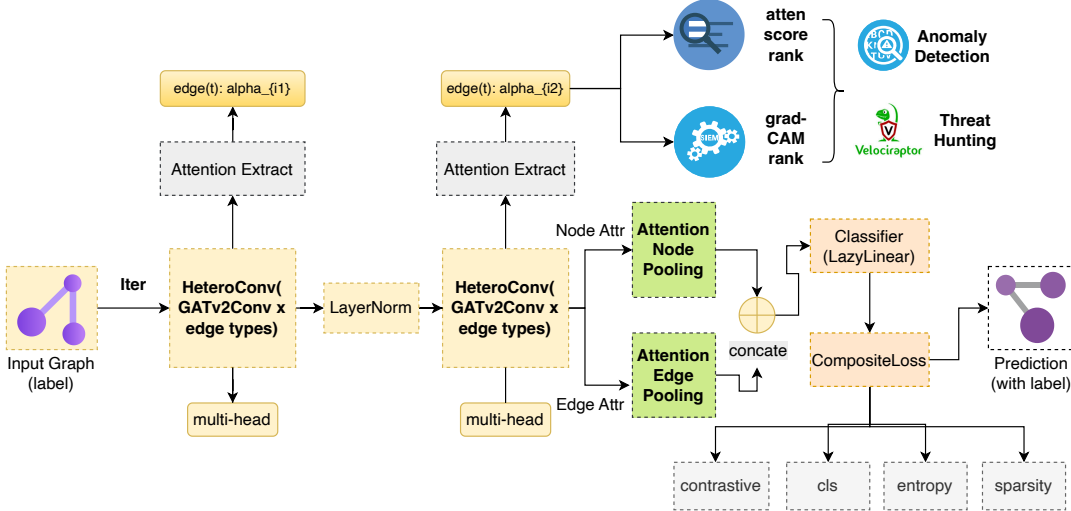


Figure 3: HeteroGAT-Rank Framework

**Why these components.** Each term targets a distinct failure mode observed in practice: removing  $\mathcal{L}_{\text{contras}}$  reduces embedding separability and generalization across ecosystems; removing  $\mathcal{L}_{\text{entropy}}$  makes attention diffuse and explanations unstable; removing  $\mathcal{L}_{\text{sparsity}}$  leads to overly large subgraphs that are less actionable. We do not include additional objectives (e.g., reconstruction losses) because our input graphs are already structured behavioral abstractions; adding generative terms increased training cost without improving detection or explanation quality in our preliminary trials.

**Hyperparameters and stability.** We set small weights for the regularizers ( $\lambda_{\text{ent}} = \lambda_{\text{sp}} = 0.01$ ) to prevent regularization terms from dominating gradients early in training. This stabilizes optimization (avoids occasional gradient spikes) and improves convergence speed while preserving feature saliency in the learned explanations.

**3.3.4 Attention Extraction.** We further equip the model with a dual attention extraction module for post-hoc interpretation and ranking: Attention-based Ranking and Grad-CAM-based Ranking.

**Attention-based Ranking.** In order to enhance the interpretability of our heterogeneous graph model, we implement an attention-based ranking mechanism that operates on edge-level and node-level attention coefficients generated by multi-head GATv2 layers. Let  $a_{ij}^{(k)}$  denote the attention coefficient from source node  $j$  to target node  $i$  under attention head  $k$ . These scores are aggregated across heads (e.g., via mean pooling) to produce a single importance score  $\bar{\alpha}_{ij}$  for each edge:  $\bar{\alpha}_{ij} = \frac{1}{K} \sum_{k=1}^K a_{ij}^{(k)}$ . In the implementation, edges are sorted according to their aggregated attention scores, and the top- $k$  most salient ones are extracted.

Each top-ranked edge is tracked back to its source and target nodes, and optionally filtered based on edge type and node attributes. These top elements serve a dual purpose: (i) they act as interpretable subgraph components that reveal what the model focuses on for prediction, and (ii) simultaneously serve as pooled representations for downstream tasks such as classification.

**Grad-CAM-based Ranking.** To complement attention saliency, we compute a gradient-based influence signal with respect to attention weights and use gradient magnitude as an *influence proxy* for ranking. Concretely, after a backward pass, we aggregate per-head gradient magnitudes for each edge and select top- $k$  edges/nodes accordingly. This sensitivity-based view complements raw attention scores and helps surface runtime elements that most affect the prediction, without claiming causal explanations. As our one-hop setting focuses on behavioral evidence, the extracted top-ranked nodes/edges correspond to concrete runtime actions that support behavioral comprehension and operational triage.

### 3.4 Scalability and Efficiency

Training heterogeneous GNNs on ecosystem-scale behavioral graphs is constrained by (i) host memory for feature encoding/graph materialization and (ii) GPU memory/time for pooling and attention. Our dataset totals 10M+ nodes and 54M+ edges, with highly skewed per-instance edge cardinalities (e.g., Action edges up to 128,781), making naive loading and dense tensorization impractical. To keep the pipeline feasible and reproducible, we apply implementation-level optimizations summarized in Table 2: we use HuggingFace Accelerate [14] for multi-GPU training and stream serialized subgraphs per mini-batch via a custom DataLoader. For encoding, Ray Actor [24]-hosted stateful encoders avoid repeated initialization and reduce memory duplication (89GB  $\rightarrow$  <50GB). On the GPU side, sparsity-aware pooling/attention avoids dense representations under edge-type skew, and we enable attention/edge-level interpretability extraction only when needed to reduce overhead.

## 4 Differential Analysis

Differential analysis in this work aims to identify the most influential structural and semantic components within heterogeneous

**Table 2: Observed impact of engineering optimizations.**

Optimization	Impact / rationale
Stateful feature encoders (Ray Actors)	Reduces peak host memory from 89 GB to < 50 GB by avoiding encoder duplication and repeated initialization across workers.
Streaming subgraph materialization	Materializes only the current mini-batch; preloading all subgraphs is infeasible at our scale.
Sparse ops for pooling/attention	Avoids dense tensorization under extreme edge-type skew (e.g., Action edges up to 128,781), reducing GPU memory pressure and making computation practical.

graphs that drive prediction behaviors. This is particularly important in security-focused dependency graphs, where software packages—regardless of their ecosystem origin (e.g., Python, Node.js, Java)—exhibit diverse patterns of runtime behavior, risk propagation, and graph topology.

Our methodology leverages attention mechanisms from graph neural networks, specifically masked GATs, to quantify feature importance at the node and edge level. Let  $\alpha_{(u,v)}^\tau$  represent the learned attention score for edge  $(u,v)$  of type  $\tau$ . These attention weights function as interpretable proxies for feature salience, offering insights at both global and context-specific levels of analysis.

#### 4.1 Global Feature Ranking

Feature ranking synthesizes attention-based signals across the entire graph, which identifies nodes with high cumulative attention across all graphs:  $\text{Score}_v = \sum_{(u,v) \in \mathcal{E}} \alpha_{(u,v)}^\tau$ . To prevent deterministic overfitting and improve ranking robustness, controlled Gaussian noise is added. The full implementation is provided in Algorithm 1:

---

##### Algorithm 1 Differential Feature Ranking

---

```

Require: Attention Weights  $\alpha$ , Edge Index Map  $E$ , Top- $k$  value  $k$ , Noise Factor  $\eta$ 
Ensure: Ranked nodes and edges:  $\mathcal{N}^*$ ,  $\mathcal{E}^*$ 
1: for all edge types  $e_t$  in  $\alpha$  do
2:   Compute mean attention score:  $\bar{\alpha}_{e_t} \leftarrow \text{mean}(\alpha_{e_t})$ 
3:   Add Gaussian noise:  $\bar{\alpha}_{e_t} \leftarrow \bar{\alpha}_{e_t} + \mathcal{N}(0, \eta)$ 
4:   Sort  $\bar{\alpha}_{e_t}$  and select top- $k$  edges  $\mathcal{E}_{e_t}^*$ 
5: end for
6: Aggregate attention to each target node across all edge types
7: Select top- $k$  nodes  $\mathcal{N}^*$ 
8: Filter  $\mathcal{E}^* \leftarrow \{(u, v) \in \bigcup \mathcal{E}_{e_t}^* \mid u, v \in \mathcal{N}^*\}$ 
9: return  $\mathcal{N}^*$ ,  $\mathcal{E}^*$ 

```

---

By combining attention-based importance and gradient-guided refinement, this framework supports differential analysis with interpretability, robustness, and granularity. It provides a principled method to detect behavior signatures and attribute model decisions to specific structural patterns.

#### 4.2 Reliability Analysis

To evaluate the reliability of extracted features, we conduct complementary validations with CVE Count, and Semantic Match.

**CVE Linkage (weak external validity):** We map surfaced features to packages using lightweight name-level heuristics and query public vulnerability databases via mitrecve [38]. Because

runtime tokens are often paths/hosts rather than canonical package identifiers, and version information is not consistently available from traces, we do not resolve exact name@version matches. Therefore, the reported CVE counts should be interpreted as a *weak, lower-bound external validity signal* for relative comparison across methods, rather than a ground-truth measurement of vulnerability.

**Semantic and Trend-based Validation:** To further validate semantic reliability, we align extracted features with two complementary knowledge sources: (a) threat trend indicators from IOC data [41], and (b) descriptive text from CVE reports. Both validations quantify semantic consistency by computing the weighted similarity between model features and external knowledge entities.

Formally, for each feature  $f_i$  with importance weight  $w_i$ , its similarity  $s_{ij}$  to an external reference  $r_j$  (e.g., trend label or description embedding), and the reference frequency  $c_j$ , we define a unified reliability score:  $\sum_{i=1}^n \sum_{j=1}^m w_i \cdot s_{ij} \cdot c_j$ . This formulation captures whether highly ranked features align with prevalent and semantically relevant threat patterns. Specifically, IOC metrics (`attack_type`, `trigger_mechanism`, `malicious_function`, and `hide_method`) represent behavioral trends, while CVE descriptions (embedded using Sentence-BERT [32] and clustered via Agglomerative Clustering [25]) provide textual grounding.

## 5 Evaluation

We evaluate HeteroGAT-Rank from three operationally relevant perspectives: (1) **predictive performance** for malicious package detection, (2) **practicality** in terms of scalability and resource cost, and (3) **actionability** of surfaced runtime indicators for human triage. Because no prior work matches our exact setting—*cross-ecosystem detection from sandboxed runtime behavior traces represented as heterogeneous subgraphs*—we adopt a start-of-the-practice protocol that combines lightweight baselines, model ablations, and system-level measurements.

#### 5.1 Start-of-the-Practice Baselines and Model Variants

We compare three variants of our approach (Table 3) to isolate the impact of architectural and objective choices. **HeteroGAT** uses GATConv with global mean pooling and a standard classification loss. **DHeteroGAT** replaces the convolution with GATv2Conv and introduces attention pooling with interpretability regularizers (entropy + sparsity). **PNHeteroGAT** further adds a contrastive term to improve representation separation under cross-ecosystem variability. In addition, we include lightweight baselines that reflect common start-of-the-practice choices when only coarse statistics or token-level scoring are used:

**Entropy-based Analysis (Entropy).** We rank individual tokens (e.g., paths/domains/commands) by class-conditional entropy [30]. This yields an efficient value-level specificity signal, but ignores relational structure and cannot model interactions among behaviors.

**Correlation Analysis (Corr).** We compute Pearson correlation [37] between handcrafted global statistics (e.g., write counts, unique domains, command frequencies) and labels. This is lightweight but limited to linear dependencies and coarse feature summaries.

**Table 3: Comparison of Model Design**

Model	Conv Model	Agg. Method	Loss Function	Optimize
HeteroGAT	GATConv	Global Mean Pool	CLS	-
DHeteroGAT	GATv2Conv	Attention Pool	CLS + Entropy + Sparsity	Vector Search
PNHeteroGAT	GATv2Conv	Attention Pool	CLS + Entropy + Sparsity + Contrastive	Vector Search

*SHAP + XGBoost (SHAP).* We train an XGBoost classifier on global subgraph statistics and apply SHapley Additive exPlanations(SHAP) [6, 22]. This provides model-agnostic attributions over coarse features, but does not expose instance-level relational evidence and can be expensive at scale.

## 5.2 Predictive Performance and Ablations

**Predictive performance (sanity check).** We report standard classification metrics (Acc/Precision/Recall/F1) together with AUC (Table 4). Because labels are imbalanced across ecosystems, AUC provides a threshold-invariant view, while threshold-dependent metrics reflect a chosen operating point. We use a fixed protocol (seed, batch size 24, test ratio 0.2, threshold 0.5) for a fair comparison.

**Operational interpretation.** Our objective is not to optimize a single detection metric, but to learn representations that support *analyst-in-the-loop triage* and *pivot generation* from noisy runtime traces. Accordingly, variants with higher recall but lower precision/F1 under the default threshold can still be desirable as a *high-recall filter*, while AUC confirms that the learned signals remain discriminative. We therefore treat Table 4 as a sanity check and focus subsequent evaluation on ranking-oriented evidence (e.g., top- $k$  indicators in Table 6), which better reflects hunting utility and workload reduction.

**Table 4: Predictive performance (sanity check).**

Model	Acc	Precision	Recall	F1 Score	AUC
HeteroGAT	0.9120	0.8612	0.7412	0.7967	0.9529
DHeteroGAT	0.5062	0.3128	0.9510	0.4708	0.7265
PNHeteroGAT	0.7140	0.4105	0.5344	0.4644	0.7360
HeteroGAT*	0.8938	0.9076	0.5989	0.7213	0.9488
DHeteroGAT*	0.5108	0.3149	0.9510	0.4731	0.7234
PNHeteroGAT*	0.7135	0.4125	0.5543	0.4730	0.7362

**Resource cost.** To assess operational feasibility, we report peak host memory, peak GPU usage/reservation, and end-to-end runtime under the same 15-epoch budget (Table 5). For lightweight baselines (Entropy/Corr/SHAP), “Time” refers to scoring/explanation runtime (no GNN training).

**Table 5: Evaluation of Resource Cost (15 epochs)**

Model Type	Peak Mem (MB)	Peak GPU Usage	Peak GPU Reserve	Time
Entropy	24,691	0	0	7m7s
Correlation	195	0	0	0.06s
SHAP+XGB.	402	0	0	1.19s
HeteroGAT	338,839	29,104	33,888	26h0m47s
DHeteroGAT	332,798	25,161	29,484	12h47m44s
PNHeteroGAT	333,533	25,161	29,114	11h52m3s
HeteroGAT*	671,366	57,950	67,304	15h21m40s
DHeteroGAT*	667,176	50,344	59,016	10h37m29s
PNHeteroGAT*	668,820	50,340	58,228	10h31m35s

*Notes on variants.* Auxiliary objectives (e.g., *entropy/sparsity/contrastive*) intentionally bias the operating point toward sensitivity; under imbalance, this can increase recall at the expense of precision. Distributed runs (marked with \* in Table 5) mainly affect runtime rather than predictive quality; small metric differences can arise from nondeterminism in parallel execution.

## 5.3 System Scalability and Resource Cost

We evaluate practicality using convergence behavior and resource usage. Figure 4 shows training loss across model variants. Although DHeteroGAT and PNHeteroGAT include additional objective terms, they reach a stable regime in fewer epochs than HeteroGAT in our configuration.

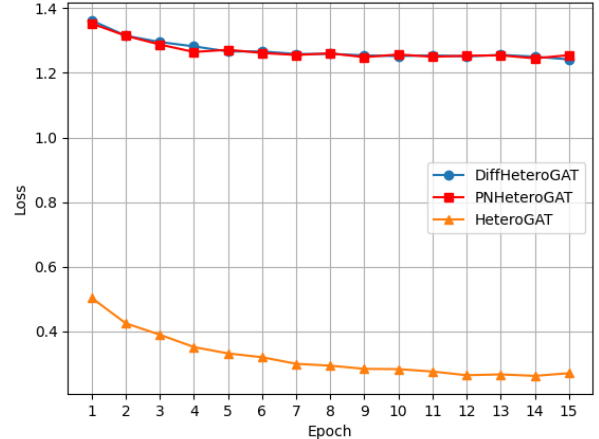
**Figure 4: Training Loss Comparison Across Models**

Table 5 reports peak host memory, peak GPU usage/reservation, and end-to-end training time for 15 epochs. We report GPU memory in MB as provided by the runtime monitor. The distributed setup roughly doubles GPU memory due to replication across two GPUs, but reduces end-to-end training time substantially (e.g., 26h→15h for HeteroGAT), demonstrating the practical benefit of parallelization for large-scale training.

## 5.4 Surfaced Runtime Indicators

We assess operational usefulness by analyzing the top- $K$  surfaced indicators ( $K = 10$ ) produced by different methods (Table 6). Here, an *indicator* is a concrete runtime entity (e.g., a path, filename, domain/host, or command) that can be inspected directly or translated into hunting queries.

As shown in Table 6, Corr and SHAP operate on global statistics, so their outputs are predominantly *counts* (screening signals), not instance-level evidence. Entropy ranks individual tokens by class-conditional entropy; scores are normalized within-method for presentation, and ties are common (thus multiple tokens may appear with score 1.0). HeteroGAT-based models surface *typed runtime entities* that also exist as nodes/edges in our graph schema, making them directly usable as pivots during triage.

*Key takeaways for analyst-in-the-loop triage.* (1) **Coarse base-lines (Corr/SHAP) are fast but weak pivots.** As shown in Table 6, Corr/SHAP primarily surface aggregate counts (e.g., `file_write_count`, `cmd_total_count`, `socket_unique_ips`). These features help screen high-activity runs, but they do not expose *which* concrete paths or filenames drove the signal, limiting instance-level investigation.

(2) **Entropy highlights token-level specificity but lacks interaction context and prioritization resolution.** Entropy surfaces specific artifacts (Table 6, Entropy row), yet it ranks tokens independently and does not leverage typed interaction context in our graphs (e.g., whether a token was `read/write/delete`, or what other behaviors co-occur around it). Moreover, ties are common after within-method normalization (multiple 1.0 scores), which reduces its usefulness for prioritizing investigations.

(3) **HeteroGAT-based models surface actionable entity-level pivots and support pivot-chain investigation.** Compared with coarse counts, HeteroGAT variants surface concrete entities that analysts can immediately inspect, especially path/filename artifacts (e.g., `/tmp` and build/cache tokens in the HeteroGAT row, and file-level artifacts such as `custom/trap.js` and `maps/package.json` in DHeteroGAT/PNHeteroGAT). While Table 6 lists entities only, the same attention-weighted graph representation enables analysts to recover each entity’s interaction context from the underlying trace/graph (action type and co-occurring neighbors), which is necessary for forming investigation-ready pivot chains.

*Feature perspective.* Across our results, HeteroGAT tends to surface path-centric indicators (e.g., ephemeral install/build artifacts such as `tmp/pip-ephem-wheel-cache-*` and random `/tmp` tokens), whereas DHeteroGAT/PNHeteroGAT increasingly emphasize filename- and dependency-level artifacts (e.g., `custom/*.js`, Babel helper files under `helpers/*`, and recognizable packages such as `@google-cloud/storage` and `end-of-stream`). PNHeteroGAT additionally surfaces `package.json` explicitly (`maps/package.json`), which aligns with known supply-chain abuse patterns in the NPM ecosystem [10, 11].

*Practitioner interpretation.* The surfaced entities are best treated as *triage pivots* rather than standalone IOCs. We observe four recurring pivot categories, each illustrated by examples in Table 6:

(i) **Ephemeral install/build artifacts (often surfaced by HeteroGAT).** Tokens such as `tmp/pip-ephem-wheel-cache-*` and short

random `/tmp` paths are common during installation and builds, but become suspicious when the surrounding trace/graph shows `write/delete` bursts, creation of executable-looking artifacts, persistence to user-scoped directories, or close temporal proximity to outbound communication. Practically, analysts pivot from the token to its action type and neighboring entities in the same run.

(ii) **Ecosystem metadata and entry-point cues.** Metadata artifacts such as `package.json` are actionable not by presence alone, but by the *runtime interactions around them* and the script-driven behaviors they can trigger. In our traces, `package.json`-related pivots typically co-occur (when observable in logs) with one or more of the following patterns that analysts can validate quickly by inspecting the same run context: (a) install-time hook execution, (b) metadata-to-execution linkage (subsequent file drops/edits), and (c) anomalous execution patterns.

(iii) **Adversarially chosen filenames/paths (e.g., `custom/trap.js`, `custom/zalgo.js`).** These artifacts can indicate loader stubs or obfuscation scaffolding [34, 39, 46], but can also appear in benign codebases. A practical check is whether they are subsequently executed/loaded and whether adjacent artifacts suggest code generation, self-modification, or interpreter one-liners.

(iv) **Popularity-based masquerading cues (e.g., recognizable dependency names).** Attackers frequently mimic or leverage popular packages in open-source ecosystems (e.g., via typosquatting or by compromising widely used dependencies [26]), which means familiar names are not sufficient evidence of benignness [27, 44]. Their operational value is strongest when they are unexpected for the package’s stated purpose or when their neighborhood shows install-time side effects; analysts should pivot to surrounding behaviors rather than flagging the name alone.

*Example pivot chain and scope.* A concrete example consistent with public reports is `audit-vue@1.6.2` associated with APT activity [9]. The package declares an install-time hook (e.g., `"postinstall": "node/main.js"`), which triggers install-time execution. In our graph schema, the analyst-facing evidence is not the semantic diff inside `package.json`, but the surrounding runtime footprint in the same sandbox run: co-occurring execution events, file reads/writes under user-scoped directories, and (when present) outbound activity to remote endpoints. This is the kind of pivot chain practitioners can validate quickly from sandbox logs and telemetry.

*Reliability signals.* DHeteroGAT and PNHeteroGAT match the highest number of CVEs (186) under our package-level name mapping, suggesting their surfaced entities are more frequently linkable to known vulnerable components. Conversely, HeteroGAT achieves the highest trend alignment score and the highest description score, indicating stronger consistency with external threat-trend indicators and CVE-description semantics. Taken together, these complementary signals suggest that the surfaced entities are both operationally actionable (entity-level pivots) and semantically grounded (external alignment), under the known limits of coarse CVE linkage.

**Table 6: Top-10 Feature Comparison and Reliability Across Methods**

Method	Top-10 Features (Ordered by Score)	CVE Count	Trend Score	Desc Score
Entropy	Readline/readline-i.ri (1.0), libxml/xmlstring.h (1.0), ClassMethods/commands-i.ri (1.0), bundler/plugin (1.0), Color/set_color-i.ri (1.0), HiddenCommand/cdesc-HiddenCommand.ri (1.0), Thor/Base (1.0), templates/newgem (1.0), Actions/inject_into_class-i.ri (1.0), source/git (1.0)	87	321296.46	111.67
Correlation	socket_unique_ips (0.3601), socket_unique_hostnames (0.2438), file_write_count (0.2249), file_unique_paths (0.2187), dns_unique_types (0.1866), dns_total_queries (0.1290), dns_unique_hosts (0.1287), file_read_count (0.1199), cmd_total_count (0.1128), cmd_unique_commands (0.1072)	-	183639.36	61.21
SHAP+XGB.	file_write_count (3.5599), cmd_total_envs (3.0887), cmd_total_count (1.1815), file_delete_count (0.9520), file_unique_paths (0.8559), cmd_total_args (0.8450), cmd_unique_commands (0.7696), file_read_count (0.4057), socket_unique_ips (0.2414), dns_unique_hosts (0.1003)	-	251627.71	62.65
HeteroGAT	tmp/pip-ephem-wheel-cache-e2vc_lpv (0.8477), simple/fakerv2 (0.1155), fakerv2_1.0 (0.1100), python3bin/analyze-python.py-version1.0installfakerv2 (0.0482), tmp/lcggeydu (0.0392), Aix/FfiHelper (0.0032), FfiHelper/address_to_string-c.ri (0.0016), FfiHelper/log-c.ri (0.0015), FfiHelper/read_interfaces-c.ri (0.0015), FfiHelper/read_load_averages-c.ri (0.0012)	1	452163.18	189.75
DHeteroGAT	custom/zalgo.js (0.0775), helpers/assertThisInitialized.js (0.0579), helpers/arrayWithHoles.js (0.0477), custom/trap.js (0.0122), @google-cloud/storage (0.0013), maps/america.js (0.0003), storage/CHANGELOG.md (0.0001), node_modules/end-of-stream (0.0001), end-of-stream/LICENSE (0.0001), sns/sns.provider.js (0.0001)	186	289148.79	114.84
PNHeteroGAT	custom/zalgo.js (0.0676), helpers/arrayWithHoles.js (0.0559), helpers/assertThisInitialized.js (0.0489), custom/trap.js (0.0233), storage/CHANGELOG.md (0.0014), node_modules/end-of-stream (0.0014), end-of-stream/LICENSE (0.0014), maps/america.js (0.0007), maps/package.json (0.0007), maps/rainbow.js (0.0007)	186	286844.12	121.86

Scores are normalized within each method. CVE Count uses package-level name mapping (version not resolved).

## 6 Operational Use Cases

HeteroGAT-Rank represents each package as a one-hop subgraph and produces a ranked list of behavioral artifacts (e.g., paths, commands, DNS hosts, and socket endpoints) as *actionable pivots* for investigation. The scenarios below are incident-driven, workflow-based case studies informed by prior operational practice, illustrating how these pivots support analyst-in-the-loop triage and integration with downstream tools.

### 6.1 Analyst Triage Workflow

As illustrated in Table 6, ranked nodes and edges provide a compact “behavioral fingerprint” for each package. Analysts can quickly inspect dominant runtime actions (file access, command execution, DNS, socket usage) to differentiate benign patterns from suspicious ones. This supports behavioral comprehension without reconstructing full program control flow.

A concise triage workflow is:

- **Inspect top-ranked nodes and edges.** Review the highest-ranked entities and their edge types (e.g., Action, DNS, CMD).
- **Pivot in telemetry.** Use surfaced entities (domains, commands, paths) as queries for IOC/telemetry search in monitoring systems.
- **Validate hypotheses.** Correlate these pivots with sandbox logs and package metadata to confirm whether behaviors are expected or suspicious.

*From indicators to hunting pivots.* In practice, analysts often operationalize high-salience artifacts into hunting pivots (e.g., install scripts, suspicious domains, and metadata files). Our surfaced entities are consistent with artifacts highlighted in public supply-chain writeups, such as `package.json` in NPM multi-stage attacks [10, 11, 35] and reported malicious modification campaigns

involving specific packages [43]. These citations are provided as contextual examples.

### 6.2 Threat Hunting Automation

Ranked behavioral entities can be exported into machine-readable rules and queries, enabling large-scale hunting in forensics and monitoring platforms (e.g., Velociraptor [15], ELK Stack [40]). This supports cross-ecosystem hunting by correlating suspicious DNS requests, file modifications, and command executions at scale.

### 6.3 Continuous Learning Loop

As more labels or analyst-confirmed incidents become available, surfaced indicators can be used to train lightweight downstream detectors [2] and to prioritize new samples for re-training [16]. This forms a feedback loop where human triage informs detection rules and model updates, improving robustness against evolving supply-chain behaviors.

## 7 Discussion

### 7.1 Lessons Learned

*L1: Operational value comes from pivots, not perfect attribution.* In industrial workflows, the primary value of HeteroGAT-Rank is that it surfaces a short, inspectable list of runtime entities (paths, commands, domains, sockets) that analysts can immediately pivot on in logs and telemetry. This is reflected in our top-K analysis (Table 6): coarse baselines largely return aggregated statistics (counts, uniques) that are useful for screening but provide limited instance-level evidence, whereas HeteroGAT-based models surface concrete artifacts (e.g., specific domains/paths/filenames) that can be directly validated in the trace and translated into hunting queries. We therefore treat attention-based ranking and gradient-based salience as practical influence signals for prioritization, rather than claiming

minimal causal explanations, which are expensive and difficult to validate at this scale.

*L2: One-hop subgraphs are a pragmatic sweet spot.* Restricting each package to a one-hop, star-shaped subgraph yields a compact “behavioral fingerprint” that is easy to store, batch, and explain. While this abstraction does not model multi-hop control/data flow, it matches the unit of evidence commonly available in sandbox/telemetry pipelines: direct interactions between a package and its environment. Importantly, the one-hop design also keeps the explanation surface interpretable (a ranked list of environment interactions rather than complex path reasoning) and avoids the compute blow-ups associated with large, skewed per-instance event volumes (see the resource and training-time costs in Table 5).

*L3: Cost and reproducibility matter as much as accuracy.* Training on heterogeneous runtime graphs can be dominated by preprocessing and data movement. Our experience shows that decoupling graph construction from model training, using lazy loading, and enabling distributed execution are necessary to make the pipeline tractable under limited GPU memory while keeping the end-to-end process reproducible. In practice, end-to-end training time and engineering overhead (Table 5) can be more decision-relevant than small metric differences, because operational adoption depends on whether the workflow can be run routinely and reliably.

*L4: Cross-ecosystem modeling reduces shortcuts, but requires careful reporting.* Pooling ecosystems encourages the model to focus on behavior patterns that transfer (e.g., installation-time script execution and suspicious outbound requests) rather than ecosystem identity. At the same time, ecosystem skew and label imbalance can distort threshold-dependent metrics and perceived performance. We therefore recommend reporting threshold-invariant metrics (e.g., AUC) alongside operationally meaningful outcomes (e.g., top-K pivot usefulness) to avoid over-interpreting raw accuracy.

## 7.2 Limitations and Threats to Validity

*Sandbox coverage and fidelity.* Our evidence is based on sandboxed execution traces collected by running packages in isolated environments (install/import phases). Behaviors that are dormant, environment-gated, time-bombed, or triggered only under specific inputs may not appear in the traces. Therefore, the surfaced indicators should be interpreted as *observed behavioral footprints under the sandbox configuration*, not a complete behavioral guarantee.

*Label imbalance and ecosystem skew.* The dataset exhibits substantial imbalance across ecosystems. Although we avoid using ecosystem identifiers as predictive features and emphasize cross-ecosystem learning, skew can still influence decision thresholds and perceived performance. Results should be interpreted together with imbalance-aware metrics and the operational goal of surfacing useful pivots.

*Explanation scope (faithfulness vs. causality).* HeteroGAT-Rank provides intrinsic explanations aligned with the model’s internal reasoning (attention ranking and Grad-CAM-style weighting). We do not claim these are minimal causal feature sets, nor do we report counterfactual evaluations, as generating valid interventions over

heterogeneous graphs at this scale is computationally prohibitive and methodologically challenging [29].

*Evaluation scope and generality.* This work targets an industrially relevant setting where organizations must triage supply-chain risk using *runtime evidence* (sandbox traces and telemetry) rather than assuming source-code availability. Our evaluation therefore emphasizes operationally meaningful improvements: (i) feasibility at scale via measured resource and training time costs (Table 5), and (ii) actionable, instance-level pivots (ranked domains/commands/paths) that can be exported into hunting queries and integrated with common forensics/monitoring stacks. We expect the approach to generalize beyond our dataset when comparable sandbox or telemetry traces are available, since the graph schema and indicator types (file, command, DNS, socket) are ecosystem-agnostic and align with standard security investigation practices.

**Practical generality checklist.** Practitioners can apply the approach beyond our dataset when comparable runtime traces are available. Concretely, deployment requires: (i) a per-package execution unit (e.g., sandbox run, CI execution, or monitored install/import), (ii) a minimal set of observable event types: file path + access mode, DNS query (host + type), socket endpoint (host/IP + port), and command strings, and (iii) a deterministic mapping from events to the one-hop graph schema. Platform differences (Linux/macOS/Windows) can be handled by normalizing path formats and by mapping equivalent telemetry sources (e.g., EDR process/file/network events) into the same event types. The method is less effective when behaviors are dormant (environment-gated or time-bombed), when critical actions occur purely in memory without observable file/network artifacts, or when sandbox policy blocks the very interactions needed to surface pivots.

## 8 Conclusion

Graph-based security analysis often depends on static code representations and therefore provides limited visibility into runtime behaviors, especially when source code is incomplete or unavailable. HeteroGAT-Rank addresses this gap by modeling each software instance as a one-hop heterogeneous subgraph constructed from sandboxed execution traces, and by producing a ranked set of interpretable runtime indicators (paths, commands, DNS hosts, and socket artifacts). This design prioritizes operational actionability: the surfaced indicators function as investigation pivots that help analysts triage suspicious packages, formulate hypotheses, and translate model outputs into hunting queries.

Future work will focus on: (1) improving explanation usability by pruning or grouping long-tail entities to produce even more compact summaries; (2) expanding ecosystem coverage and behavioral diversity to strengthen robustness under distribution shift; and (3) integrating indicator export more tightly with threat-hunting pipelines to enable near-real-time triage and feedback-driven model updates. Ultimately, we aim to make behavioral graph learning a practical bridge between automated detection and human-centered security investigation.

## Acknowledgments

This work was supported by industrial funding from JUMPSEC Ltd.

## References

- [1] [n. d.]. Anonymized Repository: DDGRL-2C32. Anonymous GitHub (4open.science). <https://anonymous.4open.science/r/DDGRL-2C32/> Accessed: 2026-01-11.
- [2] Mahdi Bahaghagh, Majid Ghasemi, and Figen Ozen. 2023. A high-accuracy phishing website detection method based on machine learning. *Journal of Information Security and Applications* 77 (2023), 103553. doi:10.1016/j.jisa.2023.103553
- [3] Frederick Barr-Smith, Tim Blazytko, Richard Baker, and Ivan Martinovic. 2022. Exorcist: Automated Differential Analysis to Detect Compromises in Closed-Source Software Supply Chains. In *Proceedings of the 2022 ACM Workshop on Software Supply Chain Offensive Research and Ecosystem Defenses* (Los Angeles, CA, USA) (SCORED '22). Association for Computing Machinery, 51–61. doi:10.1145/3560835.3564550
- [4] Piotr Bojanowski, Edouard Grave, Armand Joulin, and Tomas Mikolov. 2017. Enriching Word Vectors with Subword Information. *Transactions of the Association for Computational Linguistics* 5 (06 2017), 135–146. doi:10.1162/tacl\_a\_00051
- [5] Shaked Brody, Uri Alon, and Eran Yahav. 2022. How Attentive are Graph Attention Networks? International Conference on Learning Representations.
- [6] Tianqi Chen and Carlos Guestrin. 2016. XGBoost: A Scalable Tree Boosting System. In *Proceedings of the 22nd ACM SIGKDD International Conference on Knowledge Discovery and Data Mining (KDD '16)*. ACM, 785–794. doi:10.1145/293972.2939785
- [7] Matthias Fey and Jan Eric Lenssen. 2019. Fast Graph Representation Learning with PyTorch Geometric. arXiv:1903.02428 [cs.LG] <https://arxiv.org/abs/1903.02428>
- [8] Fabian Niklas Froh, Matias Federico Gobbi, and Johannes Kinder. 2023. Differential Static Analysis for Detecting Malicious Updates to Open Source Packages. In *Proceedings of the 2023 Workshop on Software Supply Chain Offensive Research and Ecosystem Defenses*. ACM, Copenhagen Denmark, 41–49. doi:10.1145/3605770.3625211
- [9] Yehuda Gelb. 2023. Lazarus Group Launches First Open Source Supply Chain Attacks Targeting Crypto Sector. <https://medium.com/checkmarx-security/lazarus-group-launches-first-open-source-supply-chain-attacks-targeting-crypto-sector-cabc626e404e>
- [10] Yehuda Gelb. 2023. An Ongoing Open Source Attack Reveals Roots Dating Back to 2021. <https://medium.com/checkmarx-security/an-ongoing-open-source-attack-reveals-roots-dating-back-to-2021-4a511979fd98> Accessed: 2025-07-07.
- [11] Yehuda Gelb. 2023. Python Packages Leverage GitHub to Deploy Fileless Malware. <https://checkmarx.com/blog/python-packages-leverage-github-to-deploy-fileless-malware/> Accessed: 2025-07-07.
- [12] Daniele Grattarola, Daniele Zambon, Filippo Maria Bianchi, and Cesare Alippi. 2024. Understanding Pooling in Graph Neural Networks. *IEEE Transactions on Neural Networks and Learning Systems* 35, 2 (2024), 2708–2718. doi:10.1109/TNNLS.2022.3190922
- [13] OpenSSF Securing Critical Projects Working Group. 2024. Package Analysis – open source packages behaviour sandbox. <https://github.com/ossf/package-analysis> Accessed: 2025-10-20.
- [14] Sylvain Gugger, Lysandre Debut, Thomas Wolf, Philipp Schmid, Zachary Mueller, Sourab Mangrulkar, Marc Sun, and Benjamin Bossan. 2022. Accelerate: Training and inference at scale made simple, efficient and adaptable. <https://github.com/huggingface/accelerate>.
- [15] Adam Harwood. 2023. Using Velociraptor for large-scale endpoint visibility and rapid threat hunting. <https://www.pentestpartners.com/security-blog/using-velociraptor-for-large-scale-endpoint-visibility-and-rapid-threat-hunting/>. Accessed: 2025-10-16.
- [16] Jianguo He, Runyu Mao, Zeman Shao, and Fengqing Zhu. 2020. Incremental Learning in Online Scenario . In *2020 IEEE/CVF Conference on Computer Vision and Pattern Recognition (CVPR)*. IEEE Computer Society, Los Alamitos, CA, USA, 13923–13932. doi:10.1109/CVPR42600.2020.01394
- [17] Xuehai Jia, Junwei Du, Minying Fang, Hao Liu, Yuying Li, and Feng Jiang. 2025. Vulnerability detection with graph enhancement and global dependency representation learning. *Automated Software Engineering* 32, 1 (May 2025), 14. doi:10.1007/s10515-024-00484-3
- [18] Zian Jia, Yun Xiong, Yuhong Nan, Yao Zhang, Jinjing Zhao, and Mi Wen. 2024. MAGIC: Detecting Advanced Persistent Threats via Masked Graph Representation Learning. In *33rd USENIX Security Symposium, USENIX Security 2024*. USENIX.
- [19] Baoxiang Jiang, Tristan Bilot, Nour El Madhoun, Khalidoun Al Agha, Anis Zouaoui, Shahrear Iqbal, Xueyuan Han, and Thomas Pasquier. 2025. ORTHRUS: Achieving High Quality of Attribution in Provenance-based Intrusion Detection Systems. In *Security Symposium (USENIX Sec'25)*. USENIX, USENIX.
- [20] Chen Liang, Qiang Wei, Zirui Jiang, Yisen Wang, and Jiang Du. 2024. A Source Code Vulnerability Detection Method Based on Adaptive Graph Neural Networks. In *Proceedings of the 39th IEEE/ACM International Conference on Automated Software Engineering Workshops* (Sacramento, CA, USA) (ASEW '24). Association for Computing Machinery, New York, NY, USA, 187–196. doi:10.1145/3691621.3694950
- [21] Guilong Lu, Xiaolin Ju, Xiang Chen, Wenlong Pei, and Zhilong Cai. 2024. GRACE: Empowering LLM-based software vulnerability detection with graph structure and in-context learning. *Journal of Systems and Software* 212 (2024), 112031. doi:10.1016/j.jss.2024.112031
- [22] Scott M. Lundberg and Su-In Lee. 2017. A unified approach to interpreting model predictions. In *Proceedings of the 31st International Conference on Neural Information Processing Systems* (Long Beach, California, USA) (NIPS'17). Curran Associates Inc., Red Hook, NY, USA, 4768–4777.
- [23] Chuan Luo, Sizhao Wang, Tianrui Li, Hongmei Chen, Jiancheng Lv, and Zhang Yi. 2023. RHDOFS: A Distributed Online Algorithm Towards Scalable Streaming Feature Selection. *IEEE Transactions on Parallel and Distributed Systems* 34 (2023), 1830–1847. doi:10.1109/TPDS.2023.3265974
- [24] Philipp Moritz, Robert Nishihara, Stephanie Wang, Alexey Tumanov, Richard Liaw, Eric Liang, Melih Elibol, Zongheng Yang, William Paul, Michael I. Jordan, and Ion Stoica. 2018. Ray: A Distributed Framework for Emerging AI Applications. arXiv:1712.05889 [cs.DC] <https://arxiv.org/abs/1712.05889>
- [25] Daniel Müllner. 2011. Modern hierarchical, agglomerative clustering algorithms. arXiv:1109.2378 [stat.ML] <https://arxiv.org/abs/1109.2378>
- [26] Marc Ohm, Hendrik Plate, Arnold Sykosch, and Michael Meier. 2020. Backstabber's Knife Collection: A Review of Open Source Software Supply Chain Attacks. In *Detection of Intrusions and Malware, and Vulnerability Assessment: 17th International Conference, DIMVA 2020, Lisbon, Portugal, June 24–26, 2020, Proceedings* (Lisbon, Portugal). Springer-Verlag, Berlin, Heidelberg, 23–43. doi:10.1007/978-3-030-52683-2\_2
- [27] Kush Pandya. 2025. 10 npm Typosquatted Packages Deploy Multi-Stage Credential Harvester. Socket Blog (Research Security News). <https://socket.dev/blog/10-npm-typosquatted-packages-deploy-credential-harvester> Accessed: 2026-01-11.
- [28] Jeffrey Pennington, Richard Socher, and Christopher Manning. 2014. GloVe: Global Vectors for Word Representation. In *Proceedings of the 2014 Conference on Empirical Methods in Natural Language Processing (EMNLP)*. Alessandro Moschitti, Bo Pang, and Walter Daelemans (Eds.). Association for Computational Linguistics, Doha, Qatar, 1532–1543. doi:10.3115/v1/D14-1162
- [29] Mario Alfonso Prado-Romero, Bardh Prenkaj, Giovanni Stilo, and Fosca Giannotti. 2024. A Survey on Graph Counterfactual Explanations: Definitions, Methods, Evaluation, and Research Challenges. *ACM Comput. Surv.* 56, 7, Article 171 (April 2024), 37 pages. doi:10.1145/3618105
- [30] J. R. Quinlan. 1986. Induction of decision trees. *Machine Learning* 1, 1 (1986), 81–106. doi:10.1007/BF00116251
- [31] Jakub Reha, Giulio Lovisotto, Michele Russo, Alessio Gravina, and Claas Grohfeldt. 2023. Anomaly Detection in Continuous-Time Temporal Provenance Graphs. In *Temporal Graph Learning Workshop @ NeurIPS 2023*. MIT Press. <https://openreview.net/forum?id=88tGlxhsf>
- [32] Nils Reimers and Iryna Gurevych. 2019. Sentence-BERT: Sentence Embeddings using Siamese BERT-Networks. arXiv:1908.10084 [cs.CL] <https://arxiv.org/abs/1908.10084>
- [33] Jiafeng Ren and Rong Geng. 2025. Provenance-based APT campaigns detection via masked graph representation learning. *Computers & Security* 148 (Jan. 2025), 104159. doi:10.1016/j.cose.2024.104159
- [34] Kunlun Ren, Weizhong Qiang, Yueming Wu, Yi Zhou, Deqing Zou, and Hai Jin. 2023. An Empirical Study on the Effects of Obfuscation on Static Machine Learning-Based Malicious JavaScript Detectors. In *Proceedings of the 32nd ACM SIGSOFT International Symposium on Software Testing and Analysis* (Seattle, WA, USA) (ISSTA 2023). Association for Computing Machinery, New York, NY, USA, 1420–1432. doi:10.1145/3597926.3598146
- [35] Checkmarx Security Research. 2024. An Ongoing Open Source Attack Reveals Roots Dating Back to 2021. <https://zero.checkmarx.com/an-ongoing-open-source-attack-reveals-roots-dating-back-to-2021-4a511979fd98> Accessed: 2025-10-15.
- [36] Muhammad Fakhrul Rozi, Tao Ban, Seiichi Ozawa, Akira Yamada, Takeshi Takahashi, and Daisuke Inoue. 2024. Securing Code With Context: Enhancing Vulnerability Detection Through Contextualized Graph Representations. *IEEE Access* 12 (2024), 142101–142126. doi:10.1109/ACCESS.2024.3467180
- [37] Patrick Schober, Christa Boer, and Lothar A. Schwarte. 2018. Correlation Coefficients: Appropriate Use and Interpretation. *Anesthesia & Analgesia* 126, 5 (May 2018), 1763–1768. doi:10.1213/ANE.0000000000002864
- [38] Shadawck. 2023. MITRE CVE API Client. <https://github.com/shadawck/mitreCVE>. Accessed: 2025-06-29.
- [39] Philippe Skolka, Cristian-Alexandru Staicu, and Michael Pradel. 2019. Anything to Hide? Studying Minified and Obfuscated Code in the Web. In *The World Wide Web Conference* (San Francisco, CA, USA) (WWW '19). Association for Computing Machinery, New York, NY, USA, 1735–1746. doi:10.1145/3308558.3313752
- [40] Kiruthiga Subramanian and Weizhi Meng. 2021. Threat Hunting Using Elastic Stack: An Evaluation. In *2021 IEEE International Conference on Service Operations and Logistics, and Informatics (SOLI)*. 1–6. doi:10.1109/SOLI54607.2021.9672347
- [41] Zhuoran Tan, Christos Anagnostopoulos, and Jeremy Singer. 2025. OSPtrack: A Labeled Dataset Targeting Simulated Execution of Open-Source Software. In *2025 IEEE/ACM 22nd International Conference on Mining Software Repositories (MSR)*. IEEE, 659–663. doi:10.1109/MSR6628.2025.00102

[42] Reinhard Tartler, Christian Dietrich, Julio Sincero, Wolfgang Schröder-Preikschat, and Daniel Lohmann. 2014. Static Analysis of Variability in System Software: The 90,000 #ifdefs Issue. In *2014 USENIX Annual Technical Conference (USENIX ATC 14)*. USENIX Association, Philadelphia, PA, 421–432. <https://www.usenix.org/conference/atc14/technical-sessions/presentation/tartler>

[43] Sysdig Security Research Team. 2024. *Malicious Modifications Detection: How Sysdig Identifies Open Source Attacks*. <https://www.sysdig.com/blog/malicious-modifications-detection-sysdig> Accessed: 2025-10-15.

[44] Lucija Valentić. 2023. Typosquatting campaign delivers r77 rootkit via npm. ReversingLabs Blog (Threat Research). <https://www.reversinglabs.com/blog/r77-rootkit-typosquatting-npm-threat-research> Accessed: 2026-01-11.

[45] Wenhui Wang, Hangbo Bao, Li Dong, Furu Wei, Nan Yang, Xiaodong Liu, Yu Wang, Jianfeng Gao, Ming Zhou, and Hsiao-Wuen Hon. 2020. MiniLM: Deep Self-Attention Distillation for Task-Agnostic Compression of Pre-Trained Transformers. In *Advances in Neural Information Processing Systems*. <https://arxiv.org/abs/2002.10957>

[46] Wei Xu, Fangfang Zhang, and Sencun Zhu. 2012. The power of obfuscation techniques in malicious JavaScript code: A measurement study. In *2012 7th International Conference on Malicious and Unwanted Software*. 9–16. doi:10.1109/MAWARE.2012.6461002

[47] Jiao Yin, Mingjian Tang, Jinli Cao, Mingshan You, Hua Wang, and Mamoun Alazab. 2023. Knowledge-Driven Cybersecurity Intelligence: Software Vulnerability Coexploitation Behavior Discovery. *IEEE Transactions on Industrial Informatics* 19, 4 (April 2023), 5593–5601. doi:10.1109/TII.2022.3192027

[48] Rex Ying, Jiaxuan You, Christopher Morris, Xiang Ren, William L. Hamilton, and Jure Leskovec. 2019. Hierarchical Graph Representation Learning with Differentiable Pooling. arXiv:1806.08804 [cs.LG]

[49] Guodong Zhang, Tianyu Yao, Jiawei Qin, Yitao Li, Qiao Ma, and Donghong Sun. 2025. CodeSAGE: A multi-feature fusion vulnerability detection approach using code attribute graphs and attention mechanisms. *Journal of Information Security and Applications* 89 (2025), 103973. doi:10.1016/j.jisa.2025.103973

[50] Tianya Zhang. 2024. Network level spatial temporal traffic forecasting with Hierarchical-Attention-LSTM. *Digital Transportation and Safety* 3, 4 (2024), 233–245. doi:10.48130/dts-0024-0021

[51] Xiaodong Zhang, Haoyu Guo, Zhiwei Zhang, Guiyuan Tang, Jun Sun, Yulong Shen, and Jianfeng Ma. 2025. Effectively Detecting Software Vulnerabilities via Leveraging Features on Program Slices. *IEEE Internet of Things Journal* 12, 7 (2025), 8033–8048. doi:10.1109/JIOT.2025.3541090

[52] Xinyi Zheng, Chen Wei, Shenao Wang, Yanjie Zhao, Peiming Gao, Yuanchao Zhang, Kailong Wang, and Haoyu Wang. 2024. Towards Robust Detection of Open Source Software Supply Chain Poisoning Attacks in Industry Environments. In *Proceedings of the 39th IEEE/ACM International Conference on Automated Software Engineering* (Sacramento, CA, USA) (ASE '24). Association for Computing Machinery, New York, NY, USA, 1990–2001. doi:10.1145/3691620.3695262